Macromolecules
ARTICLE

Macromolecules **2010**, *43*, 5749–5755 **5749**
DOI: 10.1021/ma100882w

Deuterium NMR Study of Orientational Order in Cellulosic Network Microfibers

S. Kundu,[†] G. Feio,[†,§] L. F. V. Pinto,[†] P. L. Almeida,[†,‡] J. L. Figueirinhas,*[,§,⊥] and M. H. Godinho*[,†]

[†]*CENIMAT/I3N, Departamento de Ciência dos Materiais, Faculdade de Ciências e Tecnologia, FCT, Universidade Nova de Lisboa, 2829-516 Caparica, Portugal,* [‡]*ACF−DEEA, ISEL/IPL, R. Conselheiro Emídio Navarro, 1, 1950-062 Lisboa, Portugal,* [§]*CFMC−UL, Av. Prof. Gama Pinto 2, 1649-003 Lisboa, Portugal, and* [⊥]*Departamento de Física, IST-TU-Lisbon, Av. Rovisco Pais 1, 1049-001 Lisboa, Portugal*

Received April 20, 2010; Revised Manuscript Received May 25, 2010

ABSTRACT: Deuterium NMR was used to investigate the orientational order in a composite cellulosic formed by liquid crystalline acetoxypropylcellulose (APC) and deuterated nematic 4′-pentyl-4-cyanobiphenyl (5CB-αd_2) with the percentage of 85% APC by weight. Three forms of the composite including electro spun microfibers, thin film and bulk samples were analyzed. The NMR results initially suggest two distinct scenarios, one where the 5CB-αd_2 is confined to small droplets with dimensions smaller than the magnetic coherence length and the other where the 5CB-αd_2 molecules are aligned with the APC network chains. Polarized optical microscopy (POM) from thin film samples along with all the NMR results show the presence of 5CB-αd_2 droplets in the composite systems with a nematic wetting layer at the APC-5CB-αd_2 interface that experiences an order−disorder transition driven by the polymer network N−I transition. The characterization of the APC network I−N transition shows a pronounced subcritical behavior within a heterogeneity scenario.

I. Introduction

Cellulose is the main constituent of plant cells and the mostly available polymer in nature, it is made up of β-D-glucopyranose monomers, each of which has one primary and two secondary hydroxyl groups that can undergo esterification and etherification among other chemical reactions. Introduction of substituents can make cellulose soluble in water due to the destruction of crystalline regions, which arise from the inter- and intra-hydrogen bonding among hydroxyl groups. Hydroxypropylcellulose (HPC) can generate aqueous liquid crystalline solutions and some HPC esters were found to originate thermotropic and lyotropic phases.[1−3] Thermotropic cholesteric cellulose esters were reported in literature to undergo a cholesteric-nematic transition upon shearing.[4] Besides anisotropic mechanical properties as seen in other LC polymeric materials, the cholesteric cellulose esters also present some remarkable optical characteristics.[5] It has been reported in systematic studies[6−8] that isotropic solutions of cellulose and cellulose derivatives were successfully electrospun into fibers using different cellulose derivatives and different electrospinning parameters, where "electrospinning" or electrostatic fiber spinning is a process for drawing fibers with submicrometer diameters through the action of electrostatic forces. Recently, electrospun fibers made from liquid crystalline cellulose derivatives were obtained showing a very peculiar helical twisting.[9] The expected connection between the unusual mechanical behavior and the chains director arrangement in the fibers prompted the search for the director structure in these systems.[10] Of interest is also the nematic to isotropic transition in these networks. While this transition is always weakly first order in LC of small molecules and in LC polymers, it may show different behaviors in network systems, ranging from a supercritical scenario to a discontinuous scenario depending upon the details and the history of the system.[11−13] To investigate both the molecular alignment and the molecular order in these cellulosic networks we have used deuterium NMR which is a well proven technique for this purpose. We have prepared a composite network system formed by acetoxypropylcellulose and the nematic liquid crystal 5CB-αd_2 as the deuterated probe. Besides preparing electrospun non woven fiber samples we have also produced thin film (∼50 μm thick) and bulk samples of the same material for comparison purposes. Since a deuterated probe is being used to monitor the orientational order in the composite system the question of how the probe molecules are distributed through the network must be addressed. Figure 1 shows the deuterium spectra recorded at several temperatures in the nonaligned fibers sample. Very similar spectra are also obtained in the thin film and bulk samples. These spectra in the intermediate temperature range are composed of a Pake[14] like pattern with a superimposed central isotropic peak. This indicates that the majority of the probe molecules are partially ordered but the probe director is randomly distributed in three dimensions, while a small amount of the probe molecules reside in totally disordered regions giving rise to the central narrow peak. Two distinct scenarios are compatible with these DNMR results, one where the majority of the probe molecules are uniformly distributed over the volume and are ordered by the network chains, the other where the majority of the probe molecules are concentrated in probe rich regions with dimensions smaller that the magnetic coherence length so that no magnetic field director alignment takes place.

The distinction between the two cases was achieved mainly through the evidence coming from the polarizing optical microscopy (POM) images recorded in typical thin film samples and the study of deuterium spectra obtained in a sample of aligned fibers as will be shown later. The combined evidence led us to conclude that the majority of the probe molecules are concentrated in small probe rich regions distributed over the network volume.

*Corresponding author.

Published on Web 06/11/2010

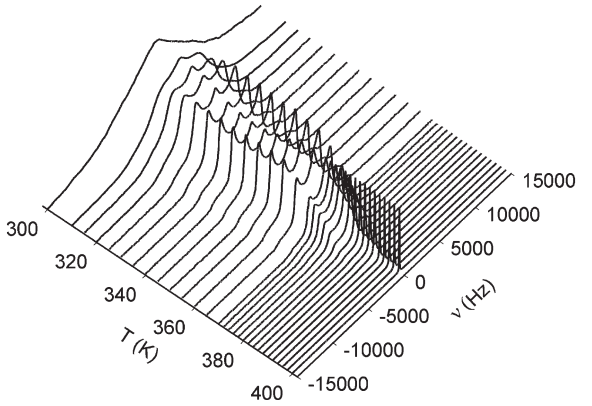

Figure 1. Deuterium spectra recorded at several temperatures in the fibers' sample. Similar spectra are obtained in the other samples studied.

The analysis of the deuterium spectra is then similar to published studies on LC confined to small cavities,[15] and allows us to obtain the order parameter imposed on the probe molecules at the network 5CB interface S_S. Considering the expected similarity between this order parameter and the network chains order parameter, we have used it to analyze the I−N transition in this network. In particular we found a pronounced subcritical behavior for the network I−N transition within a heterogeneity dominated scenario.[10−12] The spectra from the different forms of the network were successfully fit in the temperature range 320−400 K considering the order parameter S_S imposed by the network chains as determined from the minimization of a Landau−De Gennes free energy expansion up to fourth order in the order parameter describing the composite network N−I transition, with a distribution of transition temperatures.[11,12]

The deuterated probe used, 5CB-αd_2 shows a N−I transition well below the analyzed range of temperatures from 320 to 400 K. The fact that the majority of the probe molecules are partially ordered within this range as the spectra show, indicates that ordering is being imposed on the 5CB molecules within the enclosures through the 5CB-cellulose derivative interaction at the enclosures' surface. This makes the order parameter position dependent within the 5CB enclosures, since it has a null equilibrium value in bulk at these temperatures. In his work,[16,17] Ping-Sheng has shown that a liquid crystal in physical contact with a solid substrate may become partially ordered even above its nematic to isotropic transition. Following Sheng's work, several authors[15,18,19] have presented models for the order parameter characterization in confined LCs above its bulk N−I transition using deuterium NMR. Our analysis follows closely one of this works[15] allowing us to access the order parameter imposed on the 5CB molecules at the LC cellulose derivative interface based on the simulation of the D-NMR spectra.

II. Experimental Section

Acetoxypropylcellulose (APC) and the nematic liquid crystal α deurated 5CB-αd_2 have been used to produce a composite material in the form of bulk samples, thin films and micronano fibers. The synthesis of APC was performed according to the procedure previously described.[3] The acetylation of hydroxypropylcellulose (HPC) (Aldrich, nominal M_w = 100 000) (molar substitution equal to 3.85 determined by ^{1}H NMR) was performed by adding the starting material polymer (50 g) to acetic anhydride (150 mL) to give a viscous solution on standing. Acetic acid (13.5 mL) was added as a catalyst to initiate esterification. The mixture was allowed to stand for 1 week with stirring and with 4 h heating intervals at 60 °C (once per day). The polymer was poured in water and the whitish viscous solid was washed several times with water. Recrystallization of the product in THF/water afforded APC as a translucent birefringent solid (95% yield). The degree of acetylation (DA) was found to be 2.22 for this batch (evaluated by ^{1}H NMR).

The α-deuterated liquid crystal 5CB-αd_2 was obtained by an adaptation of Gray et al.[20] strategy in a three-step reaction pathway. The first step was a Friedel−Crafts reaction of pentanoyl chloride with 4-bromobipheny yielding the subsequent ketone. After reduction of the ketone with $LiAlD_4$ to afford 4-bromo-4′-(α-d_2)-pentylbiphenyl, the last step consisted in the aromatic substitution of the bromine for cyanide group in order to obtain 5CB-αd_2. This reaction was performed in a sealed tube at 240 °C with short reaction time and excellent yield (90%). The structure of newly synthesized 5CB-αd_2 was confirmed by ^{1}H NMR, ^{13}C NMR and FTIR. The N−I transition temperature was confirmed by performing polarizing optical microscopy with varying temperature. The N−I bulk transition temperature is 307 K. The solutions of [APC (85 wt %/wt) + 5CB(αd_2) (15 wt %/wt)] (70 wt %/wt) in acetone (30 wt %/wt) (Aldrich—without further purification) were produced at room temperature and the contents were allowed to mix for several weeks. After homogenization the phase separated solutions were submitted to three different processes to obtain composites in different forms. To produce the sheared films, the solutions were submitted to a shear flow mechanical field and casted onto a glass plate at room temperature with a calibrated Gardner knife moving with a controlled rate of $v = 5\ \mathrm{mm \cdot s^{-1}}$. The composite film after solvent evaporation was carefully peeled from the substrate. To produce bulk samples, the solution was poured onto a glass substrate, the solvent was allowed to evaporate and the remaining material in the form of a thick film was then carefully peeled off from the substrate. To produce the micro and nano fibers a standard electro-spinning setup was used. The solutions were poured into a 5 mL syringe fitted with a 23-gauge needle, which was then placed on the infusion syringe pump (KDS100) to control the polymer solution feed rate. A conducting ring, 15 cm diameter, was held coaxially with the needle tip at its center, and electrically connected to it. The needle and the ring were directly connected to the positive output of a high-voltage supply (Glassman EL 30 kV). After applying the electric potential between the metallic syringe-tip and the plate, the viscous anisotropic APC solution was continuously fed to the syringe-tip at a constant flow rate of 0.04 mL/h, and accelerated toward the flat grounded collector target by the ensuing electric field. The optimized operating conditions for the continuous drawing of cellulose fibers were at a voltage of 15 kV for a distance between nozzle and collector, d = 15 cm. The deposition was performed either directly onto a glass substrate, producing a nonwoven nano- and microfiber mat of nonaligned fibers, or onto a rotation substrate to obtain aligned fibers. The thickness of the thin film formed by the deposited fibers falls in the range of a few micrometers, depending upon the deposition time and the deposition conditions. The DNMR spectra were recorded on an AVANCE III Bruker NMR spectrometer equipped with a 7.049 T superconducting magnet, corresponding to a deuterium resonance frequency of 46.072 MHz. A solid echo pulse sequence with a $\pi/2$ pulse length of 4.5 μs and pulse separation of 20 μs was used in the data acquisition with a recycle delay of 0.5 s.

III. NMR Theory

A uniaxial nematic domain of single site deuterated molecules with the director at an angle θ to the static magnetic field **B** produces a deuterium spectra composed of two absorption lines centered at the *Larmor* precession frequency

$$f_L = \frac{1}{2\pi}\gamma B$$

and with a splitting given by

$$\nu = \frac{3}{2}\nu_Q S\left(\frac{3}{2}\cos^2\theta - \frac{1}{2}\right) \quad (1)$$

where ν_Q is the effective quadrupolar coupling constant of the deuterated site in the molecules and S is the nematic order parameter. The 5CB enclosures in our composite cellulosic network are smaller than the magnetic coherence length and in these enclosures the order parameter S and the local director are position dependent, $S = S(\mathbf{r})$ and $\theta = \theta(\mathbf{r})$. In the temperature range studied the equilibrium value of S in the bulk nematic is zero and its finite value within the enclosures is driven by the probe-network interaction at the enclosures' walls. Heterogeneity in the cellulosic network if present may give rise to diverse order parameter profiles in different enclosures expressed by $S_i(r)$. The fast molecular diffusion of the probe molecules within the enclosures averages the quadrupolar Hamiltonian and in the complete averaging limit, shown to be a reasonable approach in a similar situation,[15] one obtains from each enclosure a two line spectra with a splitting ν_i

$$\nu_i = \frac{3}{2}\bar{\nu}_{Qi}\left(\frac{3}{2}\cos^2\Theta - \frac{1}{2}\right) \quad (2)$$

where $\bar{\nu}_{Q\ i}$ is the motionally averaged quadrupolar coupling constant and Θ the angle between the average director in the 5CB enclosure and the external magnetic field. The diffusion averaged $\bar{\nu}_{Q\ i}$ in each enclosure is obtained as

$$\bar{\nu}_{Qi} = \left\langle \nu_Q S_i(\vec{r})\left(\frac{3}{2}\cos^2\theta_i(\vec{r}) - \frac{1}{2}\right)\right\rangle \quad (3)$$

where the brackets indicate an average over the enclosures' volume and ν_Q, S_i, and θ_i have been defined before. Over each homogeneous region (i) of the sample the average directors in the 5CB enclosures are randomly distributed and the spectrum $G_i(\omega)$ resulting from the contributions from all the enclosures in that region becomes a Pake pattern, $G_i(\omega)$ is calculated as

$$G_i(\omega) = \int_\Omega [L(\omega - \upsilon_i\pi, \delta\omega) + L(\omega + \upsilon_i\pi, \delta\omega)]P(\Omega)\,\mathrm{d}\Omega \quad (4)$$

where L is a line shape function taken as Lorentzian with width at half eight $\delta\omega$, υ_i is given by eq 2, $\Omega \equiv (\Theta,\Phi)$, $P(\Omega) = 1/(4\pi)$, and $\mathrm{d}\Omega \equiv \sin(\Theta)\,\mathrm{d}\Theta\,\mathrm{d}\Phi$. The final expression for the spectrum to be fitted to the experimental results includes the contributions from all regions (i) and is given by an weighted average of $G_i(w)$ over the distribution of the variable characterizing the heterogeneity in the system, namely the cellulosic network N−I transition temperature. A small temperature independent isotropic contribution $I(\omega)$ is also added to account for those completely disordered probe enclosures at all temperatures studied.

$$G(\omega) = \langle G_i(\omega)\rangle + I(\omega) \quad (5)$$

The spectra recorded in the composite network system contain an ordered component with a Pake shape and a superimposed isotropic central peak, as the temperature increases the relative areas change with a strengthening of the central peak, at $T =$ 400 K and above the ordered component vanishes. This progressive increase of the central peak with an increase in temperature is an indication of heterogeneity in the system, more specifically the data suggest the presence of a distribution on the I−N transition temperature in the network, a temperature increase augments the fraction of sample regions that crossed over the order to disorder transition decreasing the ordered component of the spectra.

To complete the theoretical model description we address now the specific calculation of the averages indicated in eqs 3 and 5.

Equation 3 defining the value of $\bar{\nu}_{Q_i}$ considers an averaging over the volume of the 5CB enclosures of the product $S_i(\mathbf{r})$ $P_2(\cos(\theta_i(\mathbf{r})))$, to calculate it we follow the approach considered in ref 15 where $\mathbf{S}(\mathbf{r})$ is estimated as the order parameter profile predicted in a confined system above the N−I bulk transition by the *Landau De Gennes* formalism for this transition. Within this formalism and in the one elastic constant approximation the free energy density can be written as[21]

$$f[Q] = f_o + \frac{a}{2}(T - T_p{}^*)trQ^2 - \frac{b}{3}trQ^3 + \frac{c}{4}(trQ^2)^2 + \frac{L}{2}\nabla Q\nabla Q + gtr(Q - Q_S)^2\delta(\vec{r} - \vec{r}_S) \quad (6)$$

where Q is the order parameter tensor, f_0 is the Q independent part of f, a, b, c, L, and g are positive phenomenological constants and $T_p{}^*$ is the super cooling limit of the probe isotropic phase. The last term represents the surface contribution and accounts for the 5CB- cellulosic network interaction with g quantifying its strength. Q_S is the order tensor imposed by the network at the 5CB enclosure surface located at $\mathbf{r}_s$. Because the temperature range studied is well above the N−I bulk transition temperature for 5CB, the order parameter is expected to be small and nonzero only close to the enclosure surface, besides we are only interested on the average indicated in eq 3. These factors allow us to consider extra simplifying assumptions as done in ref 15 for the determination of the order parameter profile within the enclosure that include the neglect of the third and fourth power terms in the free energy density expansion, the consideration of the nematic medium as a uniaxial medium and the approximation to a one-dimensional problem with uniform director, where the LC interacts with a flat surface located at $x = 0$.

Under these approximations the total free energy is given by the integration of a simplified form of f(Q) over the 5CB enclosure volume V,

$$F = \int_V \left(f_o + \frac{a}{2}(T - T_p{}^*)S^2(x) + \frac{L}{2}[\nabla S(x)]^2\right)\mathrm{d}V + \frac{g}{2}(S_0 - S_S)^2 A \quad (7)$$

where $S(x)$ is the nematic order parameter at a distance x from the surface, A is the enclosure's surface area, S_0 is the order parameter at the surface, and S_S is the surface imposed degree of order. The minimization of F leads to an order parameter profile $S(\mathbf{x})$ decaying exponentially with the distance to the surface

$$S(x) = S_0 e^{-x/\xi} \quad (8)$$

where ξ is the correlation length of the surface induced nematic order and is given by

$$\xi = \sqrt{\frac{L}{aT_p{}^*}}\sqrt{\frac{T_p{}^*}{T - T_p{}^*}} = \xi_0\sqrt{\frac{T_p{}^*}{T - T_p{}^*}} \quad (9)$$

with $\xi_0 \sim 0.65$ nm[22] and $T_p{}^* \sim T_{NI} - 1.1$ K[15] $= 305.9$ K . The order parameter at the surface S_0 takes the value that minimizes F and is determined by substituting $S(\mathbf{x})$ given by eq 8 back in eq 7 and minimizing F with respect to S_0. The result reads

$$S_0 = \frac{S_s}{1 + \dfrac{\sqrt{aL(T - T_p{}^*)}}{g}} \quad (10)$$

It has been shown[23] that to describe the experimental NMR results in confined systems, a modified order parameter profile is better suited than $S(\mathbf{x})$ given by 8, this modified profile is given by:

$$S(x) = \begin{cases} S_0, 0 \le x \le l_0 \\ S_0 e^{-[x-l_0]/\xi}, x > l_0 \end{cases} \quad (11)$$

where l_0 is the thickness of a region adjacent to the interface where the order parameter is uniform and equal to S_0. l_0 is a fitting parameter in the model. Regarding the angle $\theta_i(\mathbf{r})$ between the nematic director at **r** and the average director in the enclosure, we have assumed as done in ref 15 an elliptical enclosure with a bipolar director structure in the nematic layer as depicted in Figure 2, leading to an approximate value of

$$\cos(\theta_i(z)) = \sqrt{\frac{1-(z/Z_0)^2}{1-(z/Z_0)^2(1-(R_0/Z_0)^2)}} \quad (12)$$

where R_0 and Z_0 are the two distinct radius of the elliptical enclosure.

$S(x)$ given by expression 11 is also adapted to the cylindrical geometry of the elliptical enclosure

$$S(\vec{r}) = \begin{cases} S_0, l_\perp = \vec{n}_s(\vec{r}_s - \vec{r}) \le l_0 \\ S_0 e^{-[l_\perp - l_0]/\xi}, l_\perp > l_0 \end{cases} \quad (13)$$

where $l_\perp$ is the distance from the point defined by **r** to the surface of the enclosure along the surface normal $\mathbf{n_s}$. $\bar{\nu}_{Qi}$ given by eq 3 becomes explicitly

$$\bar{\nu}_{Qi} = \nu_Q \frac{1}{V}\int_V S_i(\vec{r})\left(\frac{3}{2}\cos^2\theta_i(\vec{r}) - \frac{1}{2}\right) dV = \nu_Q S_{0i} F(R_0/Z_0, l_0/Z_0, \xi/Z_0) \quad (14)$$

In the fits, the function F was evaluated numerically for specific values of its arguments; R_0/Z_0 was taken as 1 for simplicity, l_0 is a fitting parameter, and Z_0 was set at an average value of 190 nm in accord with information obtained from POM images recorded in similar APC films doped with equivalent concentrations of a cyanobiphenyl mixture. An analytical approximation for the function F is found in ref 15 .

The order parameter at the surface S_{0i} is related to the network surface induced order S_{Si} by eq 10, as we are dealing with a liquid crystalline network, S_{Si} is closely linked to the network chains order parameter and is thus temperature dependent. To model the S_{Si} temperature dependence we have considered a Landau−De Gennes (LG) free energy expansion up to fourth order in the order parameter S_{Si} for the order parameter dependent part of the network chains free energy per unit of volume,[10,11,21]

$$F = F_o + \frac{A}{2}(T - T_i^*){S_{Si}}^2 - \frac{B}{3}{S_{Si}}^3 + \frac{C}{4}{S_{Si}}^4 - GS_{Si} \quad (15)$$

where A, B, and C, are temperature independent phenomenological constants, G accounts for the possible presence of an internal stress field in the network favoring an increase in order, and T_i^* is the super cooling limit of the network isotropic phase for region i in the sample. The equilibrium value of the network chains related order parameter in region i, S_{Si} is obtained through the minimization of 15, carried out by finding the solution of the cubic eq 16 resulting from $dF/dS_{Si} = 0$ that corresponds to the lowest free energy per unit of volume. The form of the cubic eq 16 shows that the order parameter S_{Si} given by one of its three solutions is only a function of $(T - T_i^*)$ and the ratios B/A, C/A, and G/A which are fitting parameters in the model.

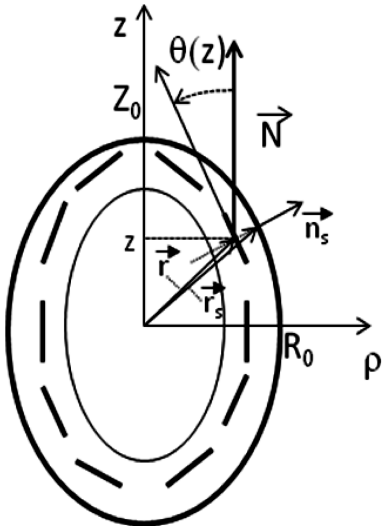

Figure 2. 5CB enclosure with the surface induced nematic layer schematically shown. **N** is the average enclosure director, and the small traces indicate the local director at each point within the nematic layer.

$$\frac{dF}{dS_{Si}} = A(T - T_i^*)S_{Si} - B{S_{Si}}^2 + C{S_{Si}}^3 - G = 0 \Rightarrow (T - T_i^*)S_{Si} - \frac{B}{A}{S_{Si}}^2 + \frac{C}{A}{S_{Si}}^3 - \frac{G}{A} = 0 \quad (16)$$

The progressive increase of the disordered component in the spectra with the increase in temperature points to the presence of heterogeneity in the system. It was included in the model by considering a Gaussian distribution in T^* temperatures over the different regions in the sample. The spectrum at each temperature given by eq 5 is calculated explicitly as

$$G(w,T) = \langle G_i(w,T)\rangle + I(w) = I(w) + \int G(w, S_S(T,T^*))\frac{e^{-(T^* - \langle T^*\rangle)^2/2{\sigma_{T^*}}^2}}{\sqrt{2\pi}\sigma_{T^*}} dT^* \quad (17)$$

where $\langle T^*\rangle$ and σ_{T^*} are respectively the average supper cooling limit temperature of the isotropic phase and its standard deviation. $G(w,T)$ given by 17 is fitted to the spectra obtained at different temperatures ranging from 310 K up to 400 K. The fitting parameters involved include $\langle T^*\rangle$ and σ_{T^*} already discussed, the ratios of the LG constants B/A, C/A, and G/A, the values l_0 and g, the relative weight of the permanent disordered component on the spectra, and the spectral line broadening $\delta\omega$ from both the ordered and the disordered components. For $\delta\omega$ of both the ordered and disordered components, a monotonous temperature dependence was considered.

IV. Results and Discussions

The spectra obtained as a function of temperature in the three samples analyzed are very similar and Figure 1 shows them for the fibers' sample. In the intermediate temperature range they are composed of a Pake like ordered component with a superimposed isotropic peak. To simulate these spectra a model was presented in the NMR Theory section that relies on the deuterated 5CB probe molecules being phase separated out of the network and concentrated in probe rich enclosures. This hypothesis is based on

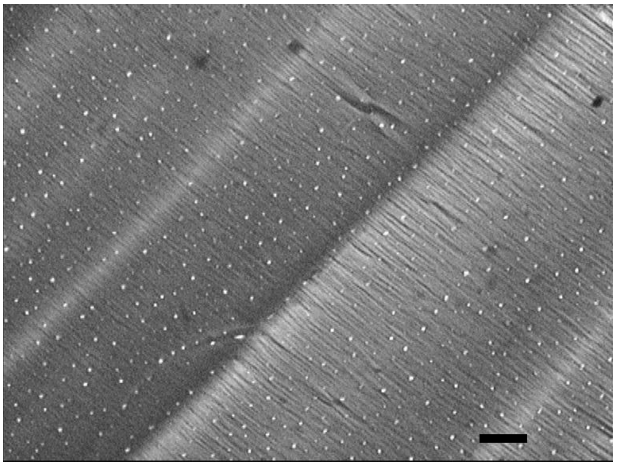

Figure 3. Typical POM image from the composite APC network thin film doped with a cyanobiphenyl mixture. The black bar is 4 μm long.

two distinct observations; one is the direct observation of POM images in similar APC composite films, as shown in Figure 3, that evidence for the presence of these enclosures.

The second observation comes from the analysis of deuterium spectra obtained in samples of aligned network fibers. These fibers produced by electro-spinning were deposited in glass lamellae carefully aligned in the electro spinning apparatus to achieve oriented fibers along an average direction labeled X. These lamellae were then stacked together and placed in a glass tube whose axis is normal to the NMR static magnetic field $\mathbf{B_0}$. The spectra obtained for two distinct orientations A and B of the fibers relative to the static magnetic field are shown in Figure 4.

In case A, the average fiber direction X is parallel to the $\mathbf{B_0}$ and in case B it is orthogonal as described in Figure 5.

The spectra shown in Figure 4, cases A and B, are very distinct, while case A constitutes a powder pattern indicating a distribution of director orientations relative to $\mathbf{B_0}$, case B is compatible with a much more uniform orientation of the directors relative to $\mathbf{B_0}$. Looking closer to the spectra, we see in case A a inner pair of peaks whose splitting is very close to half the splitting of the less pronounced outer peaks indicating in this case that there are probe directors in the sample covering the orientations from parallel to $\mathbf{B_0}$ (producing the outer peaks), to normal to it (producing the inner peaks). The central peak comes from a disordered component. In case B the splitting between the two peaks is identical to the inner peaks splitting in case A showing that in this case the directors are mainly orthogonal to $\mathbf{B_0}$. These observations are compatible with a scenario where the probe directors are mainly uniformly distributed in the XY plane. To test this hypothesis the spectra from cases A and B were simulated with expression 4 considering a distribution of director orientations uniform in the XY plane an peaked for $\theta = \pi/2$, Figure 6 shows the θ dependence of the director orientation distribution obtained from the fits. This distribution function was parametrized by a series expansion on spherical harmonics,

$$P(\theta,\phi) = \max\{\sum_{l=0}^{n}\sum_{m=-l}^{l} a_{lm} Y_l^m(\theta,\phi), 0\} \qquad (18)$$

considering only even terms in l so that $P(\theta,\phi) = P(\pi-\theta,\phi+\pi)$. Good fits were achievable with $n = 6$ and uniform dependence on ϕ. The results reported correspond to the non null fitting parameters a_{lm} having the values $a_{00} = 0.2821$, $a_{20} = -0.2368$, $a_{40} = 0.1495$, and $a_{60} = -0.05173$. The spectra and simulations are represented on Figure 4.

We can conclude that in spite of the fibers being aligned with the X direction, the probe directors are distributed uniformly

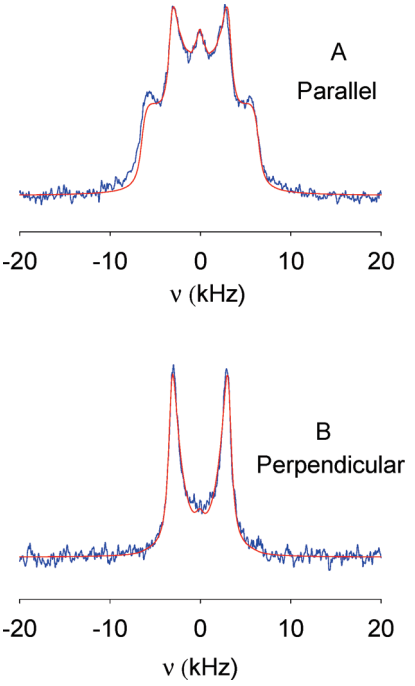

Figure 4. Deuterium spectra obtained from aligned fibers deposited in glass lamellae and recorded for two distinct orientations of the magnetic induction $\mathbf{B_0}$ relative to the fiber alignment direction. The spectra were recorded at $T = 325$ K.

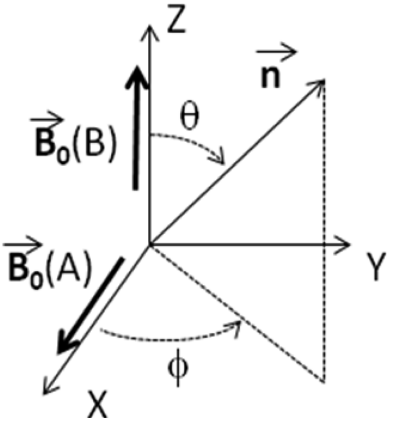

Figure 5. Description of the magnetic induction $\mathbf{B_0}$ orientation relative to the average fiber direction, along the X axis, for cases A and B.

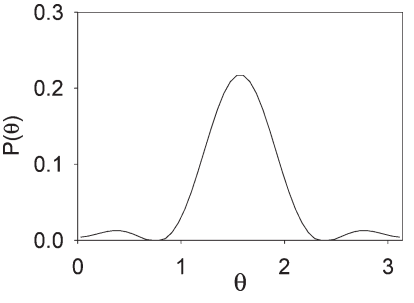

Figure 6. Distribution of director orientations in the aligned fibers sample $P(\theta,\phi) = P(\theta)$, the distribution is uniform in ϕ (see Figure 5 for angle definitions).

around the Z axis and lying predominantly in the XY plane. This alignment can only be produced by the sample preparation method and would not be achievable if the probe

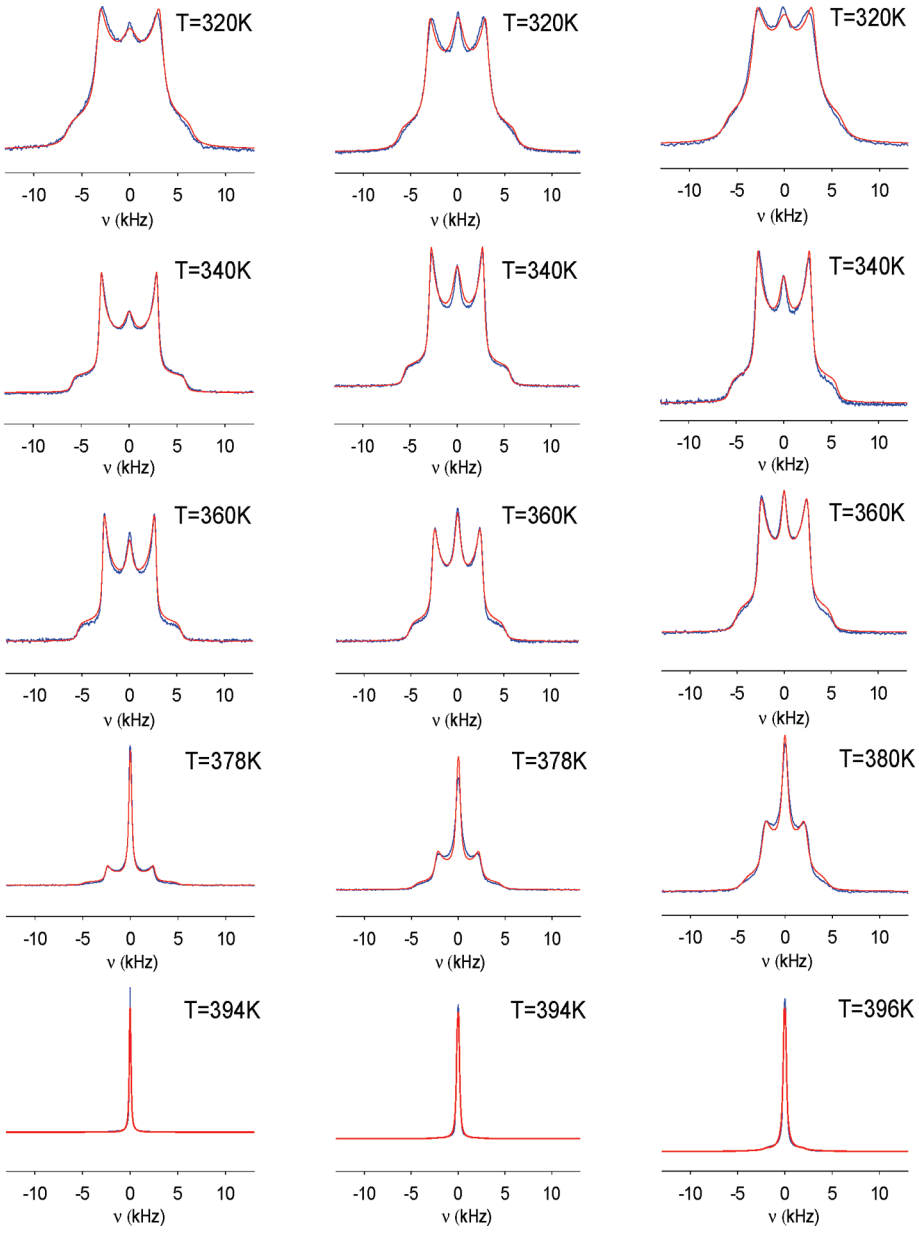

Figure 7. Model fit of the deuterium spectra obtained in the three distinct samples in the temperature range studied. From left to right, nonaligned fiber sample data, bulk sample data and film sample data.

Table 1. Values of the Fitting Parameters Considered in the Model Obtained from the Fits Shown in Figure 7[a]

sample	l_o (nm)	g (J m^{-2})	$\langle T_c \rangle$ (K)	σ_{T_c} (K)	B/A (K)	C/A (K)	G/A (K)	% permanent isotropic component	A (J K^{-1} m^{-3})
fibers	32	0.7	380	6.9	1.18×10^3	2.39×10^3	1.0	4	6.1×10^4
bulk	30	0.2	383	7.1	1.26×10^3	2.38×10^3	2.8	6.7	4.1×10^4
film	32	>0.8	387	8.0	0.86×10^3	1.97×10^3	1.4	4.5	2.9×10^4

[a] The last column reports the values of the parameter A obtained from the enthalpy change (ΔH) at the N−I transition[24] measured by DSC.

$$A = \frac{2\Delta H}{[T_C(S_{NT_c}{}^2 - S_{IT_c}{}^2)]}$$

molecules were uniformly distributed over the network in direct interaction with the network chains. We are led by these results and the previous observations to conclude that the 5CB probe molecules contributing to the spectra are concentrated within probe rich enclosures distributed over the network as considered in the model described in the Theory section.

Applying the model to the results obtained from the 3 samples and presented in Figure 1 for the case of the fibers sample, produces the fittings shown in Figure 7.

The model parameters obtained from the fits are given in Table 1 where we have used the relation[11] $T_C - T^* = (2B^3 - 27C^2G)/(9ABC)$ to report the N−I transition temperature T_C instead of T^*.

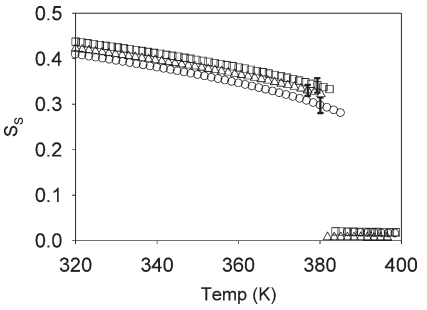

Figure 8. Temperature dependence of the order parameter S_S for $T_{Ci} = \langle T_c \rangle$ for the three distinct samples studied. Key: triangles, fibers sample; squares, bulk sample; circles, film sample. The error bars are indicated.

In Figure 8, we represent the temperature dependence of the S_s order parameter where $T_C = \langle T_{ci} \rangle$ for the three samples studied which is strongly correlated with the network chains order parameter and shows that the system is subcritical. The small order parameter values found in the three samples above T_C correspond to the best fit values but the errors affecting them indicated by the error bars do not exclude the possibility of zero order above T_C.

The spread in transition temperatures of around 7 °C obtained from the fits indicates the presence of heterogeneity in the system. Looking at the fitting parameters we find a strong 5CB-network surface interaction represented by g, significantly above the large value reported in ref 25 (1.2×10^{-2} J m^{-2}) for the interaction strength of 5CB with diacrylate based polymer fibrils in polymer network assemblies. Such values for g indicate that S_0 is very similar to Ss in the temperature range studied. We find small internal stress fields (G), well below the critical value $G_C = B^3/(27C^2)$[11] and corresponding to $0.09G_C$, $0.21G_C$, and $0.23G_C$ respectively for fibers, bulk, and film samples, giving rise to significant order changes at T_C. We find also a very low supper cooling limit with a $T_C - T^*$ difference of around 100 K. The small differences found in the order parameters temperature dependences measured in the different samples indicate that the different processing methods used do not generate relevant changes in the systems' free energy. The network chains director orientation in the electrospun fibers could not be accessed by this study because the 5CB-αd2 molecules concentrate in the enclosures and consequently are not probing the network chains director orientation.

V. Conclusions

We have used deuterium NMR to analyze the orientational order in a composite cellulosic network formed by liquid crystalline APC and a deuterated probe (5CB-αd_2), prepared in three different forms including electro spun microfibers, thin film and bulk samples. It was observed in all samples that the probe molecules phase separate out of the network and are mainly confined to small droplets. The probe molecules within the droplets become partially ordered above their bulk N−I transition temperature through the development of a nematic wetting layer at the droplet-network interface driven by the interaction with the network chains at the droplets surface. It is observed in the different systems that the droplets average director is generally random but it can become partially aligned in the fiber samples through particular preparation conditions. The temperature dependence of the network chains induced order S_s is similar for the different samples analyzed. It shows values in the range 0.29 to 0.44 below the N−I transition and 0.02 to 0.008 just above it. The APC network I−N transition is discontinuous and a significant spread in transition temperatures was found showing a subcritical behavior with the presence of heterogeneity in the system. The presence of a small internal stress field in the network responsible for a finite order above the N−I transition is also shown by the data fittings obtained in the different samples.

Acknowledgment. The authors wish to thank J. P. Canejo for the SEM image. S.K. acknowledges FCT Grant No. FRH/BPD/34096/2006. This work was partially supported by the Portuguese Science Foundation FCT through Contract Nos. PTDC/FIS/65037/2006 and PTDC/CTM/099595/2008.

References and Notes

(1) Gillbert, R. D.; Kadla, J. F. *Preparation and properties of cellulosic biocomponent fiber: Polysaccharides Structural Diversity and Functional Versatility*; Dumitriu, S., Ed.; Marcel Dekker: New York, 2005; pp 1179−1187.
(2) Werbowyj, R. S.; Gray, D. G. *Mol. Cryst. Liq. Cryst.* **1976**, *34*, 97–103.
(3) Tseng, S. L.; Valente, A.; Gray, D. G. *Macromolecules* **1981**, *14*, 715–719.
(4) Asada, T.; Toda, K.; Onogi, S. *Mol. Crysl. Liq. Crysl* **1981**, *68*, 1179–1194.
(5) Almeida, P. L.; Kundu, S.; Borges, J. P.; Godinho, M. H.; Figueirinhas, J. L. *Appl. Phys. Lett.* **2009**, *95*, 043501–043503.
(6) Viswanathan, G.; Murugesan, S.; Pushparaj, V.; Nalamasu, O.; Ajayan, P. M.; Linhardt, R. J. *Biomacromolecules* **2006**, *7*, 415–418.
(7) Kim, C. W.; Kim, D. S.; Yang, S. Y.; Marquez, M.; Joo, Y. L. *Polymer* **2006**, *47*, 5097–5107.
(8) Shukla, S.; Brinley, E.; Cho, H. J.; Seal, S. *Polymer* **2005**, *46*, 12130–12145.
(9) Canejo, J. P.; Borges, J. P.; Godinho, M. H.; Brogueira, P.; Teixeira, P. I. C.; Terentjev, E. *Adv. Mater.* **2008**, *20*, 4821–4825.
(10) Warner, M.; Terentjev, E. M. *Liquid Crystal Elastomers*; Clarendon Press: Oxford, U.K., 2003.
(11) Lebar, A.; Kutnjak, Z.; Zumer, S.; Finkelmann, H.; Sanchez-Ferrer, A.; Zalar, B. *Phys. Rev. Lett.* **2005**, *94*, 197801–197804.
(12) Cordoyiannis, G.; Lebar, A.; Zalar, B.; Zumer, S.; Finkelmann, H.; Kutnjak, Z. *Phys. Rev. Lett.* **2007**, *99*, 197801–197804.
(13) Feio, G.; Figueirinhas, J. L.; Tajbakhsh, A. R.; Terentjev, E. M. *Phys. Rev. B* **2008**, *78*, 020201–020204.
(14) Pake, G. E. *J. Chem. Phys.* **1948**, *16*, 327–336.
(15) Amimori, I.; Eakin, J. N.; Qi, J.; Skacej, G.; Zumer, S.; Crawford, G. P. *Phys. Rev. E* **2005**, *71*, 031702–031712.
(16) Sheng, P. *Phys. Rev. Lett.* **1976**, *37*, 1059–1062.
(17) Sheng, P. *Phys. Rev. A.* **1982**, *26*, 1610–1617.
(18) Crawford, G. P.; Yang, D. K.; Zumer, S.; Finotello, D.; Doane, J. W. *Phys. Rev. Lett.* **1991**, *66*, 723–726.
(19) Crawford, G. P.; Ondris-Crawford, R.; Zumer, S.; Doane, J. W. *Phys. Rev. Lett.* **1993**, *70*, 1838–1841.
(20) Gray, G. W.; Mosley, A. *Mol. Cryst. Liq. Cryst.* **1976**, *35*, 71–81.
(21) De Gennes, P.-G.; Prost, J. *The Physics of Liquid Crystals*; Clarendon Press: Oxford, U.K., 1993.
(22) Coles, H. J. *Mol. Cryst. Liq. Cryst.* **1978**, *49*, 67–74.
(23) Crawford, G. P.; Stannarius, R.; Doane, J. W. *Phys. Rev. A* **1991**, *44*, 2558–2569.
(24) Magnuson Matthew, L.; Fung, B. M.; Bayle, J. P. *Liq.Cryst.* **1995**, *19*, 823–832.
(25) Zumer, S.; Crawford, G. P. *Polymer Network Assemblies in Nematic Liquid Crystals: Liquid Crystals in Complex Geometries Formed by Polymer and Porous Networks*; Crawford, G. P., Zumer, S., Eds.; Taylor & Francis: London, 1996; pp 83−101.